Available online at www.sciencedirect.com
ScienceDirect
Journal of Organometallic Chemistry 692 (2007) 5614–5620
Journal of Organometallic Chemistry
www.elsevier.com/locate/jorganchem

Generation of Ir–Sn and Rh–Sn bonds from the oxidative addition of tin(IV) halides to $[Ir(\mu\text{-}Cl)(1,5\text{-}COD)]_2$ and $[Rh(\mu\text{-}Cl)(1,5\text{-}COD)]_2$

Joyanta Choudhury [a], D. Krishna Kumar [b], Sujit Roy [a,*]

[a] Organometallics and Catalysis Laboratory, Chemistry Department, Indian Institute of Technology, Kharagpur 721 302, India
[b] Analytical Science Discipline, Central Salt and Marine Chemicals Research Institute, Bhavnagar 364 002, Gujarat, India

Received 4 August 2007; received in revised form 19 September 2007; accepted 20 September 2007
Available online 29 September 2007

Abstract

Facile oxidative addition of $SnCl_4$, $MeSnCl_3$, and $SnBr_4$ across Ir(I) and Rh(I) cyclooctadiene complexes resulted in the formation of the corresponding Ir–Sn and Rh–Sn heterobimetallic complexes. Treatment of $SnCl_4$ with $[Ir(COD)(\mu\text{-}Cl)]_2$ and $[Rh(COD)(\mu\text{-}Cl)]_2$ afforded $[Ir(COD)(\mu\text{-}Cl)Cl(SnCl_3)]_2$ (**1**) and $[Rh(COD)(\mu\text{-}Cl)Cl(SnCl_3)]_2$ (**2**), respectively. Reaction of the organotin halide $MeSnCl_3$ with $[Ir(COD)(\mu\text{-}Cl)]_2$ led to the formation of $[Ir(COD)(\mu\text{-}Cl)Cl(MeSnCl_2)]_2$ (**3**). The reaction of $SnBr_4$ to Ir^I and Rh^I precursors gave $[Ir(COD)(\mu\text{-}Br)Br(SnBr_3)]_2$ (**4**) and $[Rh(COD)(\mu\text{-}Br)Br(SnBr_3)]_2$ (**5**) respectively, which indicates halide exchange at post-oxidative addition stage. The structures of complexes **1**–**5** were confirmed by X-ray crystallography. A *cis*-addition of Sn–X bond across Ir^I/Rh^I is proposed from the analysis of the geometrical features of "X–M–Sn" triangular units in **1**–**5**.

Keywords: Oxidative addition; Bimetallic; Iridium; Rhodium; Tin halides

1. Introduction

Complexes having transition metal-tin motif display remarkable efficacy in various homogeneous catalytic organic transformations such as hydrogenation, hydroformylation, hydrosilylation, alkene isomerization and water gas shift reaction. Accordingly there have been many-prong interests in studying such species [1]. Of the various methods available to construct such a species, the route involving an oxidative addition of a Sn–X bond to a low-valent late transition metal partner is interesting in view of the fact that it brings about desirable electronic features in the bimetallic M–Sn moiety for potential application within cooperative catalysis regime (Fig. 1) [2]. The major features which induce reactivity in such design include (i) a high-valent and soft electrophilic transition metal center for the activation of soft nucleophiles such as a π-system, (ii) a hard Lewis acidic tin center for the activation of substrates having hard donor atoms, and (iii) close proximity of M and Sn center for proximal binding and subsequent coupling between two different organic substrates [3]. Recently we have delineated success in harnessing catalytic reactivity utilizing the above concept. For example, these high-valent bimetallic complexes are found to perform efficient and highly selective electrophilic aromatic alkylation reactions with a number of electrophiles such as alcohols, esters, ethers, and aldehydes [4].

In view of the above facts, we undertook to further explore the oxidative addition of tin halides and organotin halides across low-valent late transition metal complexes of group-9. It may be noted that examples of the oxidative addition of SnX_4 or R_nSnX_{4-n} to group-10 metal complexes, chiefly platinum, and palladium are well abundant [5]. In sharp contrast, similar oxidative addition to group-9 metal complexes is relatively fewer [6], of which in only one case structural characterization by X-ray crystallography has been reported [6a]. In this article we describe the facile oxidative addition of SnX_4 (X = Cl, Br), and $MeSnCl_3$ to cyclooctadiene complexes of

* Corresponding author.
E-mail address: sroy@chem.iitkgp.ernet.in (S. Roy).

0022-328X/$ - see front matter © 2007 Elsevier B.V. All rights reserved.
doi:10.1016/j.jorganchem.2007.09.016

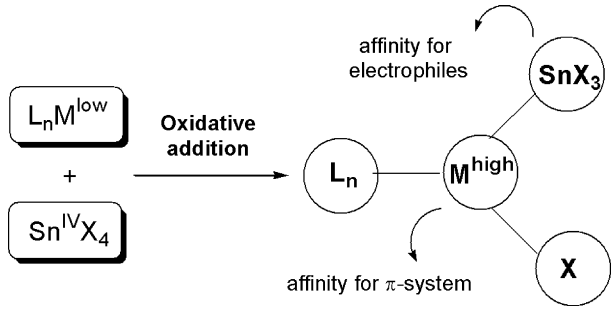

Fig. 1. Features of an M–Sn motif.

iridium(I) and rhodium(I). The study highlights the *cis*-addition pathway of Sn–X bond across Ir(I) and Rh(I).

2. Results and discussion

2.1. Reaction of SnX_4 (X = Cl, Br) and $MeSnCl_3$ with $[M(COD)(\mu\text{-}Cl)]_2$ (M = Ir, Rh) and isolation of the oxidative addition products

The reaction of the square planar $[Ir(COD)(\mu\text{-}Cl)]_2$ complex (1 equiv.) in dichloromethane with $SnCl_4$ (2.5 equiv.) in benzene at room temperature readily afforded the six-coordinate heterobimetallic complex $[Ir(COD)(\mu\text{-}Cl)Cl(SnCl_3)]_2$ **1** (Scheme 1). The rhodium(I) analog is equally effective in promoting the oxidative addition of $SnCl_4$ providing the complex $[Rh(COD)(\mu\text{-}Cl)Cl(SnCl_3)]_2$ **2** in good yield. Favorable oxidative addition of an organotin halide namely $MeSnCl_3$ across $[Ir(COD)(\mu\text{-}Cl)]_2$ gave rise to complex $[Ir(COD)(\mu\text{-}Cl)Cl(MeSnCl_2)]_2$ **3** (Scheme 2).

Interestingly both the Ir(I) and Rh(I) precursors reacted with $SnBr_4$ (2.5 equiv.) leading to the products $[M(COD)(\mu\text{-}Br)Br(SnBr_3)]_2$ (M = Ir, **4**; M = Rh, **5**) having bridging bromine atoms (Scheme 3). This observation suggests that a halogen exchange process is taking place between the initial oxidative addition product and $SnBr_4$, involving the cleavage of M–Cl bond and formation of M–Br bond. It is too early to conclude whether this process is thermodynamic or kinetic controlled, and the exact mechanism of exchange. It may be noted that Farkas et al. reported similar halo-exchange involving the formation of Pt–I bond from Pt–Cl bond in the reaction of (2,4-bis(diphenylphosphino)pentane)dichloroplatinum(II) with SnI_2 [7].

The reactions could be conducted in solvent mixtures comprising of dichloromethane/dichloroethane and

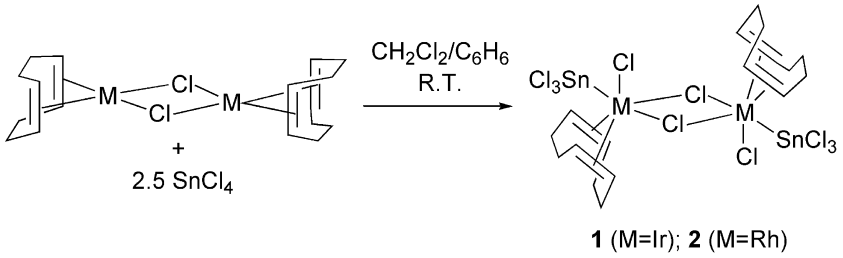

Scheme 1. Oxidative addition of $SnCl_4$ to $[M(COD)(\mu\text{-}Cl)]_2$.

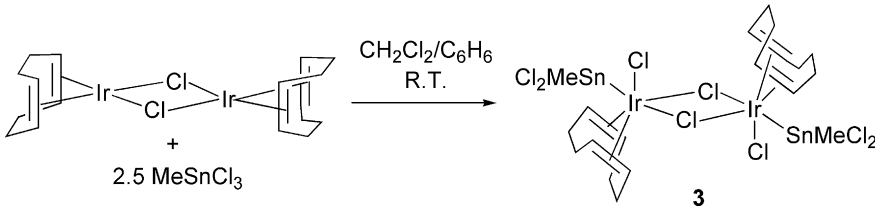

Scheme 2. Oxidative addition of $MeSnCl_3$ to $[Ir(COD)(\mu\text{-}Cl)]_2$.

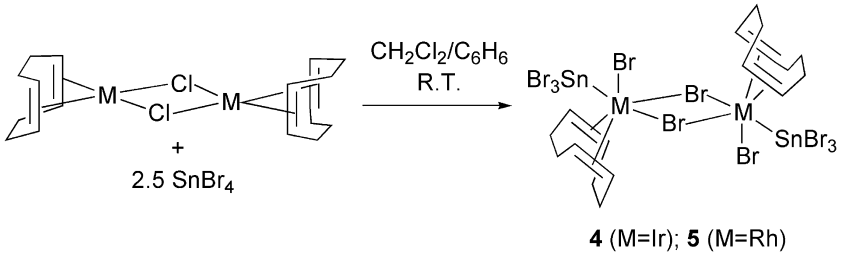

Scheme 3. Oxidative addition of $SnBr_4$ to $[M(COD)(\mu\text{-}Cl)]_2$.

benzene/toluene/xylene mixtures. Good quality single crystals could be directly obtained when reactions were conducted in absence of stirring, allowing slow diffusion of solvents. On the other hand, stirring the reaction mixture led to microcrystalline products. Complexes **1**–**5** were moderately stable in air and moisture.

The ^{1}H and ^{13}C NMR spectra of **1**–**5** in DMSO-d_6 showed characteristic peaks due to coordinated COD ligand. The resonances of $MeSnCl_2$-group in complex **3** showed upfield chemical shift at 0.93 ppm with a $^{2}J_{Sn-H}$ coupling of 65.2 Hz similar to literature value [6a]. The ^{119}Sn NMR of complex **1** and **3** showed signals at −625, and −453 ppm (with respect to Me_4Sn as external standard; negative sign indicates downfield shift). These ^{119}Sn NMR chemical shift values are well within the expected region of M–SnX_3 complexes [1a]. Due to inadequate solubility of complexes **2**, **4** and **5** the ^{119}Sn NMR could not be recorded.

2.2. Evidence in favor of cis-addition of Sn–X bond: crystal structures of *1*–*5*

The ORTEP diagrams of **1**–**5** are shown in Figs. 3–7, which illustrate that the basic structural features are similar in all cases. The immediate coordination sphere of the central iridium/rhodium atom (M) reflects a distorted octahedral geometry which is evident from a comparison of bond angles around M considering the neighboring atoms and the two centroids (axial A and equatorial B) of the olefinic bonds (Fig. 2). Most noticeable are the deviation of angles $\angle X_t^3$–M–A (by 3.93–7.80°), ∠B–M–A (4.50–4.84°), and ∠Sn–M–A (9.41–17.45°) from idealized geometry. The highly distorted tetrahedral geometry around tin center is evident from the increased ∠M–Sn–X angles (by 8.06–8.91°), and decreased ∠X–Sn–X angles (by 9.33–10.81°) from idealized geometry. The equatorial M–Sn bond length (2.578–2.596 Å) is within the normal range (2.59–2.64 Å), while the average Sn–X distance (X = Cl, 2.336 Å; X = Br, 2.467 Å) is expectedly longer than that of SnX_4. The above features are in accordance with other heterobimetallic stannyl complexes bearing cyclooctadiene ligand [6a,8,9].

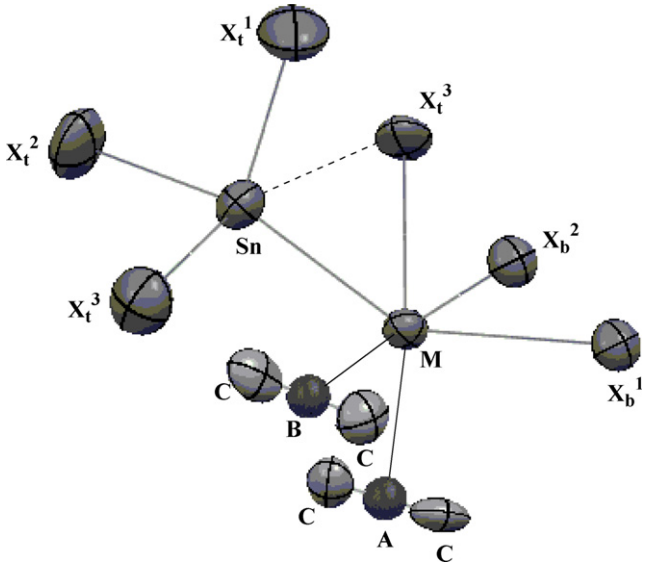

Fig. 2. Basic structural view in **1**–**5** showing the immediate coordination spheres around M and Sn. X_b = bridging halide, X_t = terminal halide, M = Ir/Rh, A and B are centroids of the two double bonds of coordinated COD ligand.

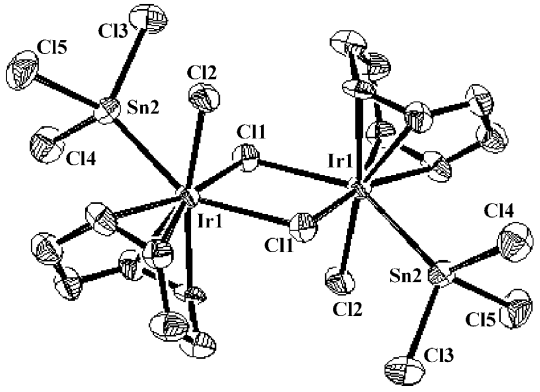

Fig. 3. Crystal structure view of **1** with 50% thermal ellipsoids (H atoms are excluded for clarity). Selected bond lengths (Å) and angles (°): Ir1–Sn2 = 2.578(4), Ir1–Cl1 = 2.545(5), Ir1–Cl1 = 2.409(6), Ir1–Cl2 = 2.385(6), Sn2–Cl3 = 2.317(5), Sn2–Cl4 = 2.350(5), Sn2–Cl5 = 2.327(5); ∠Cl1–Ir1–Sn2 = 149.57(8), ∠Cl1–Ir1–Sn2 = 81.16(17), ∠Cl2–Ir1–Cl1 = 85.56(15), ∠Cl2–Ir1–Cl1 = 93.23(14), ∠Cl1–Ir1–Cl1 = 80.88(18).

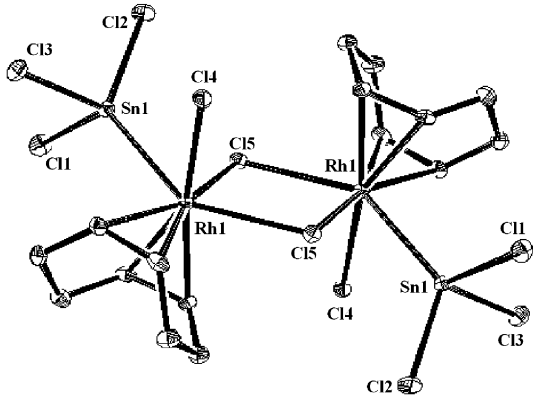

Fig. 4. Crystal structure view of **2** with 50% thermal ellipsoids (H atoms and solvent molecule are excluded for clarity). Selected bond lengths (Å) and angles (°): Rh1–Sn1 = 2.5528(4), Rh1–Cl5 = 2.6181(10), Rh1–Cl5 = 2.3939(9), Rh1–Cl4 = 2.3922(10), Sn1–Cl1 = 2.3594(10), Sn1–Cl3 = 2.3339(10), Sn1–Cl4 = 2.6854(10); ∠Cl5–Rh1–Sn1 = 145.17(2), ∠Cl5–Rh1–Sn1 = 77.75(2), ∠Cl4–Rh1–Cl5 = 92.56(3), ∠Cl4–Rh1–Cl5 = 86.79(3), ∠Cl5–Rh1–Cl5 = 82.89(3).

It is well known that the oxidative addition of metal halides E–X (E = Hg, Si, Sn, Pb) across d^8-ML_4 species may proceed by an S_N2 or a concerted pathway. The former would lead to a *trans*-disposition of E and X atoms around M, while the latter would provide a *cis*-geometry (Scheme 4, *path-a* or *path-b*) [10]. The angle ∠X–M–E is often a good indicator of the respective pathways.

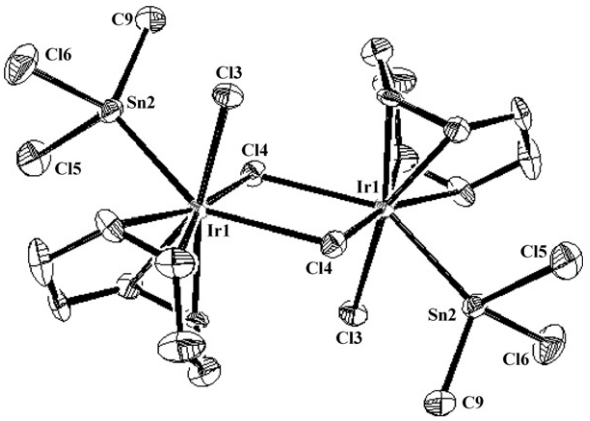

Fig. 5. Crystal structure view of **3** with 50% thermal ellipsoids (H atoms and solvent molecule are excluded for clarity). Selected bond lengths (Å) and angles (°): Ir1–Sn2 = 2.5956(14), Ir1–Cl4 = 2.594(4), Ir1–Cl4 = 2.403(4), Ir1–Cl3 = 2.371(4), Sn2–Cl5 = 2.360(4), Sn2–Cl6 = 2.328(5), Sn2–C9 = 2.134(17); ∠Cl4–Ir1–Sn2 = 147.03(8), ∠Cl4–Ir1–Sn2 = 78.18(9), ∠Cl3–Ir1–Cl4 = 93.16(13), ∠Cl3–Ir1–Cl4 = 84.74(12), ∠Cl4–Ir1–Cl4 = 80.66(12).

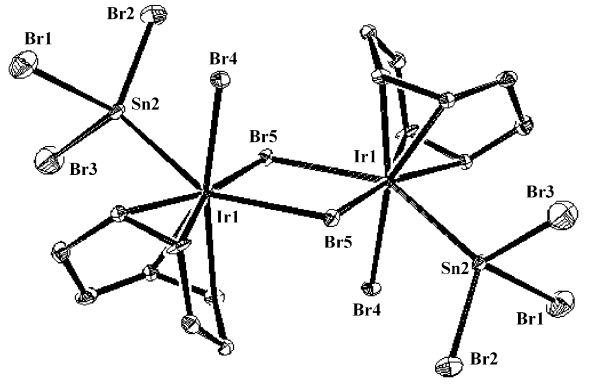

Fig. 6. Crystal structure view of **4** with 50% thermal ellipsoids (H atoms and solvent molecule are excluded for clarity). Selected bond lengths (Å) and angles (°): Ir1–Sn2 = 2.5922(12), Ir1–Br5 = 2.6435(16), Ir1–Br5 = 2.5406(16), Ir1–Br4 = 2.5179(16), Sn2–Br1 = 2.454(2), Sn2–Br2 = 2.466(2), Sn2–Br3 = 2.468(2); ∠Br5–Ir1–Sn2 = 150.24(5), ∠Br5–Ir1–Sn2 = 82.23(4), ∠Br4–Ir1–Br5 = 94.15(5), ∠Br4–Ir1–Br5 = 84.90(5), ∠Br5–Ir1–Br5 = 81.78(5).

Examination of the structures of **1**–**5** showed that in all of them the ∠X–M–Sn is far below 90°. This prompted us to closely look into the geometrical features of "X–M–Sn" triangular units in **1**–**5** and reported [Ir(COD)-(2-Me_2NCH_2–C_6H_4)(Br)$SnMe_2$Br] **6** [6a,11]. The various bond length and bond angle data of the triangular units are shown in Table 1, and the corresponding superposition plots in Fig. 8. Noticeably the non-bonded Sn···X distances are within 2.685–2.983 Å. While the distances are higher than idealized expectation for Sn–X covalent bond (2.39 Å for Sn–Cl; 2.54 Å for Sn–Br), they are well below the distances expected of van der Waals interactions (3.92 Å for Sn···Cl; 4.02 Å for Sn···Br) [12]. Therefore we assume weak but appreciable interaction between the

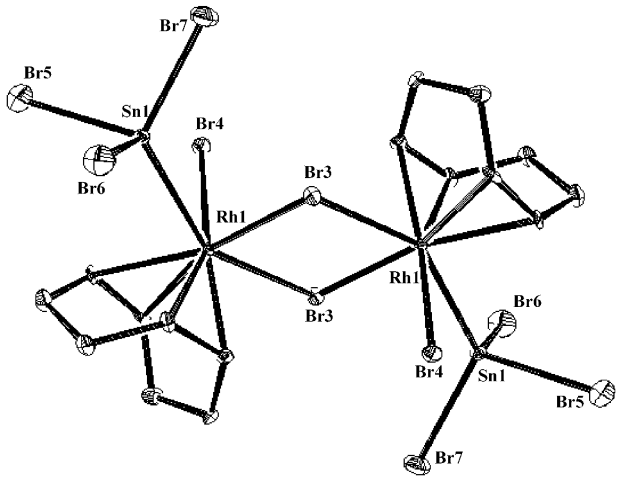

Fig. 7. Crystal structure view of **5** with 50% thermal ellipsoids (H atoms and solvent molecule are excluded for clarity). Selected bond lengths (Å) and angles (°): Rh1–Sn1 = 2.5807(8), Rh1–Br3 = 2.7283(10), Rh1–Br3 = 2.5247(10), Rh1–Br4 = 2.5157(10), Sn1–Br5 = 2.4639(12), Sn1–Br6 = 2.4805(12), Sn1–Br7 = 2.4685(11); ∠Br3–Rh1–Sn1 = 146.25(3), ∠Br3–Rh1–Sn1 = 78.81(3), ∠Br4–Rh1–Br3 = 93.96(3), ∠Br4–Rh1–Br3 = 85.39(3), ∠Br3–Rh1–Br3 = 83.56(3).

tin and halogen atoms in the triangular motifs. In our view, the above results are good indicators for the *cis*-oxidative addition (*path-b*) in the present case. Further examination of the superposition plots for "Cl–M–Sn" triangles in **1**–**3** (Fig. 8, left) reveal that a decrease in ∠Cl···Sn–M, and an increase in ∠Cl–M–Sn causes concomitant shortening of the M–Cl distance, and lengthening of the Sn···Cl distance. A similar correlation is observed in case of the "Br–M–Sn" triangular units in **4** and **5** (Fig. 8, right).

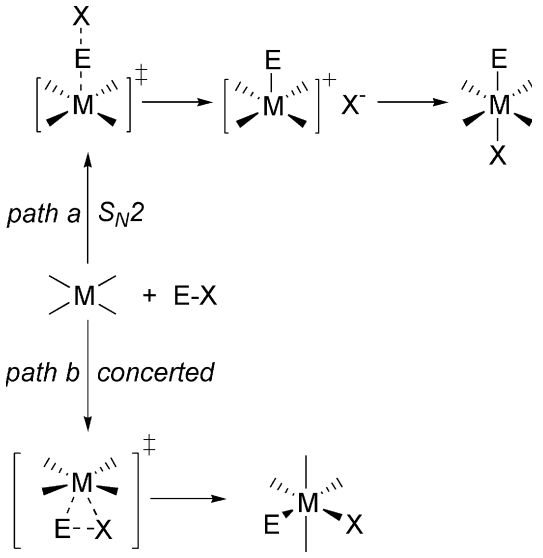

Scheme 4. Mechanism of two-electron oxidative addition of Sn–X across a transition metal center.

Table 1
Structural features of "X–M–Sn" triangular units in **1–6**[a]

Complex	X	∠Sn···X–M	∠X···Sn–M	∠X–M–Sn	Sn···X	M–Sn	M–X
1	Cl	57.47	51.21	71.32	2.892	2.578	2.385
2	Cl	60.03	54.28	65.69	2.685	2.553	2.392
3	Cl	57.80	50.63	71.57	2.910	2.596	2.371
4	Br	55.45	53.13	71.42	2.983	2.592	2.518
5	Br	57.31	55.14	67.55	2.834	2.581	2.516
6	Br	56.59	55.15	68.26	2.934	2.636	2.592

[a] Bond distances are in Å and bond angles are in degree.

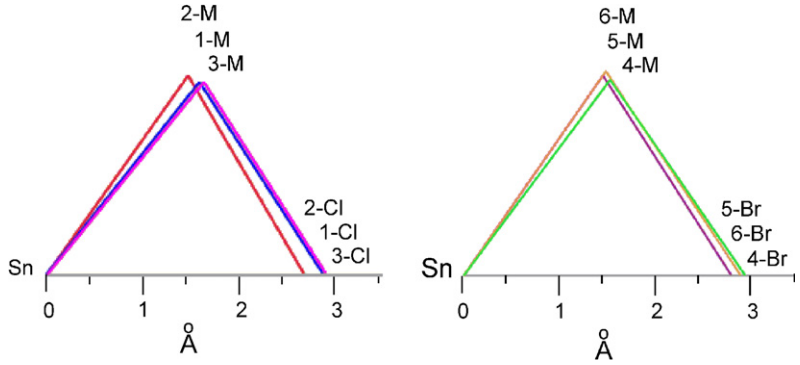

Fig. 8. Superposition plots for "Cl–M–Sn" triangles in **1–3** (left) and "Br–M–Sn" triangles in **4–6** (right). The Sn atom is at the origin and the Sn–X vector along the *x*-axis.

3. Conclusion

New "Ir–Sn" and "Rh–Sn" heterobimetallic complexes (**1–5**) were synthesized by the oxidative addition of SnX_4 and $MeSnCl_3$ reagents across Ir(I) and Rh(I) cyclooctadiene complexes and were well characterized. Facile halide exchange occurred in the reaction of $SnBr_4$ with $[M(COD)(\mu\text{-}Cl)]_2$ (M = Ir, Rh) affording bromo-bridged products **4** and **5**. A close inspection of the geometries of the resulting "X–M–Sn" triangular units in **1–5** provided evidence in favor of *cis*-addition of Sn–X bond to iridium and rhodium.

4. Experimental section

4.1. General

All preparations and manipulations have been performed under a dry oxygen free argon atmosphere using standard vacuum lines and Schlenk techniques. All solvents used for the synthesis have been dried and distilled by standard methods and previously deoxygenated in the vacuum line. ^{1}H (200, 400 MHz) and ^{13}C NMR (54.6, 100 MHz) spectra (chemical shifts referenced to signals for residual solvent) were recorded on Bruker AC 200 and Bruker Avance II 400 spectrometer at 300 K. ^{119}Sn NMR (149.2 MHz) spectra (chemical shifts referenced to signals for external tetramethyltin) were recorded in Bruker Avance II 400 spectrometer at 300 K. FTIR spectra (4000–500 cm^{-1}; KBr pellet) were obtained using a Perkin Elmer FTIR Spectrometer (Spectrum RX-I) and a Thermo Nicolet FTIR Spectrometer (NEXUS-870). Elemental analyses were performed on Perkin Elmer Instruments 2400 Series II CHNS/O Analyzer.

4.2. Synthesis of complexes *1–5*

4.2.1. *[Ir(COD)(μ-Cl)Cl(SnCl$_3$)]$_2$ (1)*

To a solution of $[Ir(COD)(\mu\text{-}Cl)]_2$ (34 mg, 0.05 mmol) in dichloromethane (3 mL) was added very slowly a solution of $SnCl_4$ (14.7 μL, 0.125 mmol) in benzene (200 μL) under an argon atmosphere. The mixture was left undisturbed for 24 h. Deep red crystals were isolated by filtration, washed with benzene and vacuum-dried. Yield: 58 mg (97%). ^{1}H NMR (200 MHz, DMSO-d_6) δ (ppm) = 1.71–1.79 (br, m, 8H, –C*H*$_2$), 2.21–2.26 (br, m, 8H, –C*H*$_2$), 4.16 (br, s, 8H, =C*H*). ^{13}C NMR (DMSO-d_6) δ (ppm) = 30.7 (–*C*H$_2$), 73.6 (=*C*H). ^{119}Sn NMR (149.2 MHz, DMSO-d_6) δ (ppm) −624. IR (KBr, cm^{-1}) 1329(s), 1433(s), 1469(m), 1617(s), 2850(w), 2907(m), 2954(m), 3010(w). Anal. Calc. for $C_{16}H_{24}Cl_{10}Sn_2Ir_2.CH_2Cl_2$: C, 15.98; H, 2.05. Found: C, 15.88; H, 2.03%.

4.2.2. *[Rh(COD)(μ-Cl)Cl(SnCl$_3$)]$_2$ (2)*

A similar method was followed using $[Rh(COD)(\mu\text{-}Cl)]_2$ (25 mg, 0.05 mmol) in dichloromethane (3 mL) and $SnCl_4$ (14.7 μL, 0.125 mmol) in benzene (200 μL). Yield: 47 mg (93%). ^{1}H NMR (200 MHz, DMSO-d_6) δ (ppm) =

1.96–2.04 (br, m, 8H, –CH_2), 2.38–2.41 (br, m, 8H, –CH_2), 4.50 (br, s, 8H, =C*H*). ^{13}C NMR (DMSO-d_6) δ (ppm) = 30.2 (–*C*H$_2$), 86.8, 87.0 (=*C*H). IR (KBr, cm^{-1}) 1303(m), 1339(s), 1450(s), 1469(m), 1612(s), 2856(w), 2870(w), 2885(w), 2910(m), 2953(m), 3016(w). Anal. Calc. for $C_{16}H_{24}Cl_{10}Sn_2Rh_2.CH_2Cl_2$: C, 18.58; H, 2.38. Found: C, 18.66; H, 2.03%.

4.2.3. *[Ir(COD)(μ-Cl)Cl(MeSnCl$_2$)]$_2$ (**3**)*

A similar method was followed using [Ir(COD)(μ-Cl)]$_2$ (34 mg, 0.05 mmol) in dichloromethane (3 mL) and MeSnCl$_3$ (30 mg, 0.125 mmol) in benzene (200 μL). Yield: 74 mg (95%). ^{1}H NMR (400 MHz, DMSO-d_6) δ (ppm) = 0.93 (s, 6H, –CH_3, ^{119}Sn satellites at 0.77 and 1.10 ppm with $^2J_{Sn-H}$ = 65.2 Hz), 1.72–1.76 (m, 8H, –CH_2), 2.22–2.24 (br, m, 8H, –CH_2), 4.15 (br, s, 8H, =C*H*). ^{13}C NMR (DMSO-d_6) δ (ppm) = 25.4 (–*C*H$_3$), 30.8 (–*C*H$_2$), 72.3 (=*C*H). ^{119}Sn NMR (149.2 MHz, DMSO-d_6) δ (ppm) −453. IR (KBr, cm^{-1}) 1303(m), 1335(s), 1430(m), 1440(s), 1452(m), 1470(m), 1617(s), 2885(m), 2911(m), 2960(s), 3020(m). Anal. Calc. for $C_{18}H_{30}Cl_8Sn_2Ir_2.CH_2Cl_2$: C, 18.45; H, 2.61. Found: C, 19.34; H, 2.59%.

4.2.4. *[Ir(COD)(μ-Br)Br(SnBr$_3$)]$_2$ (**4**)*

A similar method was followed using [Ir(COD)(μ-Cl)]$_2$ (34 mg, 0.05 mmol) in dichloromethane (3 mL) and $SnBr_4$ (16.4 μL, 0.125 mmol) in benzene (200 μL). Yield: 74 mg (95%). ^{1}H NMR (200 MHz, DMSO-d_6) δ (ppm) = 1.65–1.76 (br, m, 8H, –CH_2), 2.18–2.23 (br, m, 8H, –CH_2), 4.22 (br, s, 8H, =C*H*). ^{13}C NMR (DMSO-d_6) δ (ppm) = 30.8 (–*C*H$_2$), 73.4–73.6 (=*C*H). IR (KBr, cm^{-1}) 1337(s), 1439(s), 1468(m), 1612(s), 2857(m), 2870(s), 2910(s), 2952(s), 3016(m). Anal. Calc. for $C_{16}H_{24}Br_{10}Sn_2Ir_2.CH_2Cl_2$: C, 11.86; H, 1.52. Found: C, 12.86; H, 1.61%.

4.2.5. *[Rh(COD)(μ-Br)Br(SnBr$_3$)]$_2$ (**5**)*

A similar method was followed using [Rh(COD)(μ-Cl)]$_2$ (25 mg, 0.05 mmol) in dichloromethane (3 mL) and $SnBr_4$ (16.4 μL, 0.125 mmol) in benzene (200 μL). Yield: 64 mg (94%). ^{1}H NMR (200 MHz, DMSO-d_6) δ (ppm) = 1.86–1.94 (br, m, 8H, –CH_2), 2.29–2.40 (br, m, 8H, –CH_2), 4.52 (br, s, 8H, =C*H*). ^{13}C NMR (DMSO-d_6) δ (ppm) = 30.2 (–*C*H$_2$), 86.6, 86.8 (=*C*H). IR (KBr, cm^{-1}) 1338(s), 1431(s), 1468(s), 1618(m), 1629(m), 2830(m), 2875(m), 2940(m), 3001(m), 3021(m). Anal. Calc. for $C_{16}H_{24}Br_8Cl_2Sn_2Rh_2{\cdot}CH_2Cl_2$: C, 13.23; H, 1.70. Found: C, 13.76; H, 1.79%.

4.3. Single-crystal X–ray diffraction analysis of **1–5**

Suitable single crystals of all the complexes were obtained directly from the reaction mixture conducted with 1,2-dichloroethane/benzene (use of dichloromethane was avoided for the fast solvent-loss during data collection). The single crystal of **1** was subjected to Enraf Nonius Turbo CAD4 diffractometer with Graphite monochromated Mo Kα (λ = 0.71073 Å). Unit cell parameters were

Table 2
Crystallographic data for **1–5**

	1	**2**	**3**	**4**	**5**
CCDC No.	273475	652722	652723	652724	652725
Formula	$C_{16}H_{24}Cl_{10}Ir_2Sn_2$	$C_{18}H_{28}Cl_{12}Rh_2Sn_2$	$C_{18}H_{30}Cl_8Ir_2Sn_2$	$C_{18}H_{28}Br_{10}Cl_2Ir_2Sn_2$	$C_{18}H_{28}Br_{10}Cl_2Rh_2Sn_2$
Fw	1192.63	1113.00	1151.80	1736.18	1557.60
Temperature (K)	298	100	293	100	100
Crystal system	Triclinic	Triclinic	Triclinic	Triclinic	Triclinic
Space group	$P\bar{1}$	$P\bar{1}$	$P\bar{1}$	$P\bar{1}$	$P\bar{1}$
a (Å)	7.51(2)	7.4369(6)	7.455(4)	7.5009(15)	7.5645(8)
b (Å)	8.08(2)	8.1103(6)	8.087(5)	8.3178(17)	8.3231(8)
c (Å)	12.98(2)	12.7373(10)	12.932(8)	13.135(3)	13.0208(13)
α (°)	80.83(10)	88.1290(10)	80.940(10)	87.593(3)	87.500(2)
β (°)	83.69(10)	87.3570(10)	82.669(10)	89.190(3)	88.572(2)
γ (°)	87.54(10)	86.7380(10)	87.881(12)	86.802(3)	87.167(2)
V (Å^3)	773(3)	765.85(10)	763.6(8)	817.5(3)	817.80(14)
Z	1	1	1	1	1
ρ_c (Mg/m^3)	2.563	2.413	2.505	3.527	3.163
M (mm^{-1})	11.053	3.729	11.010	22.019	14.891
F(000)	544	530	528	774	710
θ Range (°)	1.60–24.98	1.60–26.00	1.61–24.97	1.55–26.00	1.57–28.28
Reflections collected	2953	5877	2684	7822	6971
Unique [*R*(int)]	2723 (0.0212)	2957 (0.0201)	2684 (0.0888)	3188 (0.0413)	3678 (0.0258)
Data/restraints/ parameters	2723/3/137	2957/0/154	2684/0/149	3188/0/144	3678/0/154
GOF/F^2	1.036	1.106	1.067	1.059	1.046
Final *R* indices [$I > 2\sigma(I)$]	R_1 = 0.0476, wR_2 = 0.1199	R_1 = 0.0282, wR_2 = 0.0583	R_1 = 0.0655, wR_2 = 0.1727	R_1 = 0.0601, wR_2 = 0.1600	R_1 = 0.0457, wR_2 = 0.1180
R indices (all data)	R_1 = 0.0538, wR_2 = 0.1225	R_1 = 0.0309, wR_2 = 0.0594	R_1 = 0.0705, wR_2 = 0.1767	R_1 = 0.0666, wR_2 = 0.1643	R_1 = 0.0520, wR_2 = 0.1211

obtained from a least-square refinement of 25 reflections. A standard decay of 2% was observed during the data collection. An analytical absorption correction was employed to the collected data. The structure was solved by SHELXS-97 and refined by full-matrix least squares on F^2 with SHELXL-97 methods [13,14]. The SQUEEZE function in PLATON was used to further correct the data obtained after absorption correction [15]. The non-hydrogen atoms were refined anisotropically. All calculations were performed using WINGX crystallographic software package [16]. Similarly, a suitable crystal of **3** was analyzed. Crystals of **2**, **4** and **5** were isolated from mother liquor and immediately immersed in paratone oil and then mounted. Diffraction data were collected using Mo Kα ($\lambda = 0.7107$ Å) radiation on a SMART APEX diffractometer equipped with charge-coupled device (CCD) area detector at 100 K. Data collection, data reduction [17], structure solution/refinement [13,14,18] and empirical absorption correction (SADABS) were carried out using the programs provided with the software package of SMART APEX (Bruker AXS: Madison, WI, 1999). All structures were solved by direct methods and refined in a routine manner. A summary of crystal data, details of the data collection, structure solution, and refinement for the structures are given in Table 2.

Acknowledgments

We thank the DST and the UGC, New Delhi, for fund (S.R.) and fellowship (J.C.). We also thank our collaborator Dr. P. Dastidar, CSMCRI, Bhavnagar, to allow his student (D.K.K.) to carry out the single crystal X-ray diffraction studies.

Appendix A. Supplementary material

CCDC 273475, 652722, 652723, 652724 and 652725 contain the supplementary crystallographic data for **1**, **2**, **3**, **4** and **5**. These data can be obtained free of charge from The Cambridge Crystallographic Data Centre via www.ccdc.cam.ac.uk/data_request/cif. Supplementary data associated with this article can be found, in the online version, at doi:10.1016/j.jorganchem.2007.09.016.

References

[1] (a) M.S. Holt, W.L. Wilson, J.H. Nelson, Chem. Rev. 89 (1989) 11;
(b) W. Petz, Chem. Rev. 86 (1986) 1019.
[2] (a) G.J. Rowlands, Tetrahedron 57 (2001) 1865;
(b) J.-A. Ma, D. Cahard, Angew. Chem., Int. Ed. 43 (2004) 4566.
[3] (a) R.G. Pearson, Hard and Soft Acids and Bases, DOWDEN, Stroudsburg, 1973;
(b) R.G. Pearson, Chemical Hardness, Wiley-VCH, Weinheim, 1997;
(c) S. Woodward, Tetrahedron 58 (2002) 1017;
(d) For examples of electrophilic transition metal complex, see: M. Janka, W. He, A.J. Frontier, C. Flaschenriem, R. Eisenberg, Tetrahedron 61 (2005) 6193, and references therein.
[4] (a) J. Choudhury, S. Podder, S. Roy, J. Am. Chem. Soc. 127 (2005) 6162;
(b) S. Podder, J. Choudhury, S. Roy, J. Org. Chem. 72 (2007) 3129;
(c) S. Podder, J. Choudhury, U.K. Roy, S. Roy, J. Org. Chem. 72 (2007) 3100;
(d) S. Podder, S. Roy, Tetrahedron 63 (2007) 9146;
(e) J. Choudhury, S. Roy, J. Mol. Catal. A., in press, doi:10.1016/j.molcata.2007.09.012.
[5] For a review see: J.P. Collman, W.R. Roper, Adv. Organomet. Chem. 7 (1968) 53.
[6] (a) A.A.H. van der Zeijden, G. van Koten, J.M.A. Wouters, W.F.A. Wijsmuller, D.M. Grove, W.J.J. Smeets, A.L. Spek, J. Am. Chem. Soc. 110 (1988) 5354;
(b) R. Usón, L.A. Oro, M.A. Ciriano, R. Gonzalez, J. Organomet. Chem. 205 (1981) 259;
(c) C.B. Dammann, J.L. Hughey IV, D.C. Jicha, T.J. Meyer, P.E. Rakita, T.R. Weaver, Inorg. Chem. 12 (1973) 2206;
(d) J.W. Dart, M.K. Lloyd, R. Mason, J.A. McCleverty, J. Chem. Soc., Dalton Trans. (1973) 2046;
(e) J.W. Dart, M.K. Lloyd, R. Mason, J.A. McCleverty, J. Chem. Soc., Dalton Trans. (1973) 2039;
(f) R. Kuwae, T. Tanaka, Bull. Chem. Soc. Jpn. 53 (1980) 118;
(g) A.J. Oliver, W.A.G. Graham, Inorg. Chem. 10 (1971) 1.
[7] E. Farkas, L. Kollár, M. Moret, A. Sironi, Organometallics 15 (1996) 1345.
[8] (a) M.R. Churchill, S.A. Bezman, Inorg. Chem. 11 (1972) 2243;
(b) M.R. Churchill, S.A. Bezman, Inorg. Chem. 12 (1973) 260;
(c) M.R. Churchill, S.A. Bezman, Inorg. Chem. 12 (1973) 531;
(d) P. Porta, H.M. Powel, R.J. Mawby, L.M. Venanzi, J. Chem. Soc. A (1967) 455;
(e) M.R. Churchill, K.G. Lin, J. Am. Chem. Soc. 96 (1974) 76;
(f) S. Brunie, J. Mazan, N. Langlois, H.B. Kagan, J. Organomet. Chem. 114 (1976) 225.
[9] P.T. Greene, R.F. Bryan, J. Chem. Soc. A (1970) 1696.
[10] For discussion on the mechanism of oxidative addition, see: L.M. Rendina, R.J. Puddephatt, Chem. Rev. 97 (1997) 1735.
[11] For similar "Cl–M–Sn" triangular units for M = Mo and W, see: (a) M. Elder, D. Hall, Inorg. Chem. 8 (1969) 1268;
(b) M. Elder, D. Hall, Inorg. Chem. 8 (1969) 1273;
(c) R.A. Anderson, F.W.B. Einstein, Acta Crystallogr., Sect. B: Struct. Crystallogr. Cryst. Chem. B32 (1976) 966;
(d) J.-F. Chai, L.-F. Tang, W.-L. Jia, Z.-H. Wang, J.-T. Wang X.-B. Leng, H.-G. Wang, Polyhedron 20 (2001) 3249;
(e) T. Szymańska-Buzar, T. Glowiak, I. Czeluśniak, J. Organomet. Chem. 640 (2001) 72;
(f) M. Górski, A. Kochel, I. Czeluśniak, T. Szymańska-Buzar, Inorg. Chem. Commun. 8 (2005) 202;
(g) T. Szymańska-Buzar, T. Glowiak, Polyhedron 17 (1998) 3419;
(h) T. Szymańska-Buzar, T. Glowiak, Polyhedron 16 (1997) 1599.
[12] Covalent radius (empirical) (Å): Sn, 1.40; Cl, 0.99; Br, 1.14 (taken from N.N. Greenwood, A. Earnshaw, Chemistry of the Elements, second ed., Butterworth-Heinemann, Oxford, 2005). van der Waals radius (empirical) (Å): Sn, 2.17; Cl, 1.75; Br, 1.85 (taken from A. Bondi, J. Phys. Chem. 68 (1964) 441).
[13] G.M. Sheldrick, SHELXS-97, University of Göttingen, Germany, 1997.
[14] G.M. Sheldrick, SHELXL-97, University of Göttingen, Germany, 1997.
[15] A.L. Spek, PLATON: A Multipurpose Crystallographic Tool, Ultrecht University, Ultrecht, The Netherlands, 1998.
[16] L.J. Farrugia, J. Appl. Cryst. 32 (1999) 837 (WinGX Version 1.64.05: An integrated system of windows programs for the solution, refinement and analysis of single crystal X-ray diffraction data and also Version 1.70.00).
[17] SAINT+, 6.02 ed., Bruker AXS, Madison, WI, 1999.
[18] G.M. Sheldrick, SHELXTL Reference Manual, version 5.1, Bruker AXS, Madison, WI, 1997.